Linear viscoelasticity of an inverse ferrofluid

B. J. de Gans,[1] C. Blom,[1] A. P. Philipse[2] and J. Mellema[1]
[1]*Rheology Group, Twente Institute of Mechanics, J.M. Burgers Center, Department of Applied Physics, University of Twente, P.O. Box 217, 7500 AE Enschede, The Netherlands*
[2]*Van 't Hoff Laboratory for Physical and Colloidchemistry, Debye Research Institute, University of Utrecht, Padualaan 14, 3584 CH Utrecht, The Netherlands*
(Received 12 April 1999)

A magnetorheological fluid consisting of colloidal silica spheres suspended in an organic ferrofluid is described. Its linear viscoelastic behavior as a function of frequency, magnetic field strength, and silica volume fraction was investigated with a specially designed magnetorheometer. The storage modulus G' is at least an order of magnitude larger than the loss modulus G'' at all magnetic field strengths investigated. G' does depend only weakly on frequency, and linearly on volume fraction. A model is presented for the high frequency limit of the storage modulus G'_∞. In the model our system is treated as a collection of single noninteracting chains of particles. Assuming a dipolar magnetic interaction, theory and experiment show reasonable agreement at high frequencies. [S1063-651X(99)16510-3]

PACS number(s): 82.70.Dd, 83.10.−y

I. INTRODUCTION

Magnetorheological fluids are suspensions of magnetizable particles. Their rheology can be tuned externally; in the absence of a magnetic field they behave as a liquid, whereas in an external magnetic field they behave as a solid. This is due to the formation of chains of particles as the magnetic field induces a dipole moment in each particle. Despite potential applications of magnetorheological fluids, the linear viscoelastic properties of these materials are hardly investigated. We are only aware of Kordonsky, Demchuk, and Kuzmin, [1], who have studied the magnetic field dependence of the storage modulus, using a magnetorheological fluid based on micrometer-sized iron particles.

Magnetorheological effects can also be observed in suspensions of nonmagnetic particles in a magnetic fluid or ferrofluid. In such an ''inverse'' ferrofluid, the nonmagnetic particles are typically several orders of magnitude larger than the nanosized magnetic particles that constitute the ferrofluid. Therefore, the nonmagnetic particles experience a medium that is magnetically, as well as hydrodynamically continuous. The application of a magnetic field induces a dipolar interaction between the nonmagnetic particles. The strength of the interaction can be varied either by changing the strength of the applied magnetic field or the saturation magnetization of the ferrofluid. Skjeltorp [2] studied structures and phase transitions in a two dimensionally confined inverse ferrofluid and observed the formation of particle chains when the magnetic field was directed parallel to the fluid layer.

The rheological response of inverse ferrofluids to the application of a magnetic field is orders of magnitude smaller than the response of ordinary magnetorheological fluids, based on magnetisable particles [4]. However, as nonmagnetic particles are available that are very well defined with respect to shape and size, inverse ferrofluids are very well suited for model studies of the magnetorheological effect. Unfortunately, the nonmagnetic particles used in such studies are very polydisperse [3–5]. This makes a comparison with theory difficult.

We explored the use of monodisperse silica spheres. In addition to the well defined size, the advantage of silica is the number of well documented surface modifications [6,7], allowing dispersibility of silica spheres in various organic solvents (e.g., ferrofluids). We found that stearyl alcohol–coated silica spheres are stable in ferrofluids based on oleic acid coated magnetite particles. In this paper we focus on the viscoelastic properties of this inverse ferrofluid, which were measured as a function of particle volume fraction, frequency, and magnetic field strength, using a specially designed magnetorheometer.

Theory for the viscoelasticity of magnetic fluids in the macroscopic approach assumes a bicontinuous structure consisting of magnetizable cylinders that are, in turn, assemblies of particle aggregates. The stress is calculated from the change in permeability when this structure is sheared [8,9]. This approach has the disadvantage that all information about the underlying microstructure is lost. Several authors adopt a microscopic approach based on some model for the interaction between the individual particles [10,11]. However, several effects, such as a sterically repulsive interaction and non-nearest neighbor interaction were not taken into account properly or ignored. We therefore extend the theory in Sec. II. The experimental results will be compared to the theoretical predictions in Sec. IV; details of sample preparation and the construction of the magnetorheometer are given in Sec. III.

II. CALCULATION OF THE HIGH FREQUENCY LIMIT OF THE STORAGE MODULUS

A. Assumptions

In this section we concentrate on the calculation of the high frequency limit of the storage modulus G'_∞. In this regime there is negelegible viscous dissipation, that is, $G' \gg G''$.

(i) The ferrofluid is magnetically continuous on the length scale of the radius R of the nonmagnetic particles. See Appendix A for a discussion.

(ii) The potential energy between two free particles can be written as follows:

$$U_{tot}=U_r(r)+U_d(r,\theta), \tag{1}$$

$$U_d=\frac{\mu_0\mu_r m^2}{4\pi r^3}(1-3\cos^2\theta).$$

Here m is the magnetic moment of a particle, r the center-to-center distance between two particles, θ the angle between the applied field H and the center to center vector, μ_0 the permeability of the vacuum and μ_r the relative permeability of the ferrofluid. U_r is a yet unspecified sterically repulsive potential of short range, compared to the dipolar potential. The assumption that the magnetic interaction between two particles can be modeled by the dipolar potential U_d is supported by the work of Fujita and Mamiya [12] which shows excellent agreement between calculated dipolar and measured forces between two macroscopic dipolar spheres immersed in ferrofluid.

(iii) Particles are spherical.

(iv) The stress is dominated by the contribution of the particle interactions.

(v) The structure of the suspension at rest is that of straight, gapspanning single chains, parallel to **H**. Interchain interactions are neglected. This assumption is supported by the work of Sear [13], who showed that a simple theory for noninteracting chains of particles provided a reasonable description of the behavior of a dipolar hard sphere system.

(vi) The deformation of the chains is affine.

B. Interaction forces

In this section the interaction force between two nonmagnetic spheres in a magnetized ferrofluid will be evaluated. First, a dipole moment **m** must be assigned to a nonmagnetic particle in a magnetized ferrofluid. One possibility is to solve Poisson's equation under the appropriate boundary conditions:

$$\nabla^2\Psi=\nabla\cdot\mathbf{M}. \tag{2}$$

Here **M** denotes the magnetization of the ferrofluid and Ψ denotes a scalar magnetostatic potential, for which we have $\mathbf{H}=-\nabla\Psi$. The local deviation from the externally applied, homogeneous magnetic field, as it is present in the sample, can be seen as the ''magnetic field'' of the nonmagnetic particle. From the dipolar term of this deviation the dipole moment can be calculated.

If the magnetization is either saturated or a linear function of the magnetic field then $\nabla\cdot\mathbf{M}=0$. Poisson's equation, simplifies to Laplace's equation, which can be solved analytically [14]. From now on these two situations will be referred to as the linear and the saturated regime, respectively. The expressions for **m** are

(i) *Linear regime:*

$$\mathbf{m}=-4\pi\beta R^3\mathbf{H}, \tag{3}$$

$$\beta=\frac{\mu_r-1}{2\mu_r+1},$$

(ii) *Saturated regime:*

$$\mathbf{m}=-\frac{4}{3}\pi R^3\mathbf{M}_s. \tag{4}$$

In the case of an isolated particle, **H** is simply the externally applied magnetic field as present in the sample $\mathbf{H}_0$. It equals the external magnetic field as present in air minus the (shape dependent) demagnetizing field. However, when the particles form chains, **H** will contain contributions of the other particles in the chain. To include this ''mutual induction effect'' in our expression for the magnetic moment within the linear regime we follow a treatment analogous to that of Martin and Anderson [10]. The field of a magnetic dipole can be written as

$$\mathbf{H}_d=\frac{3\hat{\mathbf{r}}(\mathbf{m}\cdot\hat{\mathbf{r}})-\mathbf{m}}{4\pi r^3}. \tag{5}$$

The self consistent magnetic moment of a dipole within an infinite chain of equally spaced particles follows from

$$\mathbf{m}=-4\pi\beta R^3[\mathbf{H}_0+2\zeta(3)\mathbf{H}_d]. \tag{6}$$

$\zeta(n)$ denotes the Riemann ζ function; it accounts for the influence of the other particles in the chain. Using polar coordinates, the various components of **m** can be found:

$$m_r=m_0\cos\theta\left(1+\frac{4R^3\beta\zeta(3)}{r^3}\right)^{-1}, \tag{7}$$

$$m_\theta=-m_0\sin\theta\left(1-\frac{2R^3\beta\zeta(3)}{r^3}\right)^{-1}. \tag{8}$$

We have set $m_0=-4\pi\beta R^3H_0$. So, in the case of an undeformed chain parallel to the magnetic field, the magnitude of the magnetic moment $m=m_r$ *decreases* because of the contribution of the dipolar fields.

Using that $\mathbf{F}=\nabla(\mathbf{m}\cdot\mathbf{B}_d)$, where B denotes the magnetic induction, and $\mathbf{B_d}=\mu_0\mu_r\mathbf{H_d}$ expressions for the interaction force between two particles can be found. Without mutual induction the force can be written as

$$\mathbf{F}_d=F_{d,r}\hat{\mathbf{r}}+F_{d,\theta}\hat{\boldsymbol{\theta}}, \tag{9}$$

$$\mathbf{F}_d=-\frac{3\mu_0\mu_r m^2}{4\pi r^4}[(3\cos^2\theta-1)\hat{\mathbf{r}}+\sin(2)\hat{\boldsymbol{\theta}}]. \tag{10}$$

As far as the magnetic moment is concerned, the expression derived for the linear and the saturated regime can both be used. If mutual induction effects are included, the magnetic moment itself is also dependent on r and θ. Assuming affine deformation, the result is

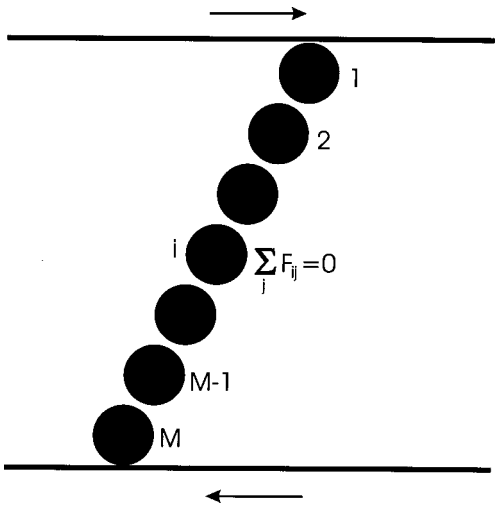

FIG. 1. *M*-particle chain under shear. The net interaction force on each particle is zero, except for the particles 1 and *M*.

$$\mathbf{F}_d=-\frac{\mu_0\mu_r}{4\pi r^4}\left\{\left[6m_r^2-3m_\theta^2-12m_r^2\left(\frac{r^3}{4\beta R^3\zeta(3)}+1\right)^{-1}-6m_\theta^2\left(\frac{r^3}{2\beta R^3\zeta(3)}-1\right)^{-1}\right]\hat{\mathbf{r}}+(4m_r^2\tan\theta+2m_\theta^2\cot\theta)\hat{\boldsymbol{\theta}}\right\}. \tag{11}$$

C. Stress tensor

The interaction contribution to the stress tensor T can be written as [15]

$$\mathsf{T}=-\frac{1}{V}\sum_{i=1}^{N}\mathbf{F}^i\mathbf{r}^i. \tag{12}$$

Here N denotes the number of particles in the volume V, $\mathbf{r}^i$ denotes the position vector and $\mathbf{F}^i$ denotes the total interaction force acting upon the particle i. We now consider an M-particle chain, as shown in Fig. 1. The forces on each particle should balance, so $\mathbf{F}^i=\mathbf{0}$ for all particles, except for the two particles, 1 and M that link the chain to the walls. Choosing the origin at the center of the Mth particle, we can write down the following expression for the stress, assuming that $M\gg 1$:

$$\mathsf{T}=-\frac{N}{V}[\zeta(4)\mathbf{F}_d^{12}\mathbf{r}^{12}+\mathbf{F}_r^{12}\mathbf{r}^{12}]. \tag{13}$$

Here $\mathbf{F}^{12}$ denotes the force that is exerted on particle 1 by particle 2. $\mathbf{r}^{12}$ denotes the vector that connects the centers of the particles 1 and 2. The factor $\zeta(4)$ accounts for the interaction of particle 1 with its non-nearest neighbors. Furthermore, we used that M times the number of chains is equal to the total number of particles N. The measured shear stress is the xy component of the asymmetric stress tensor

$$\mathsf{T}_{xy}=-\frac{N}{V}[\zeta(4)F_{d,x}^{12}r_y^{12}+F_{r,x}^{12}r_y^{12}], \tag{14}$$

from which the high frequency limit of the storage modulus G'_∞ follows:

$$G'_\infty=-\frac{dN}{V}\left[\zeta(4)\frac{\partial}{\partial\gamma}F_{d,x}^{12}\bigg|_{r=d,\theta=0}-\frac{d}{dr}U_r^{12}\bigg|_{r=d,\theta=0}\right]. \tag{15}$$

Here γ denotes the shear deformation. The equilibrium distance between two particle centers was set equal to d. Next we consider the forces acting upon particle 1 if the chain is at rest:

$$\zeta(4)F_{d,y}^{12}+F_{r,y}^{12}=\zeta(4)F_{d,r}^{12}\bigg|_{r=d,\theta=0}-\frac{d}{dr}U_r^{12}\bigg|_{r=d,\theta=0}=0. \tag{16}$$

It is assumed that, at rest, the interaction force between the wall and the first particle does not have a y component. The force exerted by the wall on the first particle is assumed to be a friction force having an x component only. Friction could be due to surface irregularities, Van der Waals forces, or hydrodynamic friction.

Equation (16) can be used to eliminate the repulsive force from Eq. (14). By doing so we arrive at the following surprisingly simple formula for G'_∞:

$$G'_\infty=-\frac{dN}{V}\zeta(4)\frac{\partial}{\partial\gamma}F_{d,\theta}^{12}\bigg|_{r=d,\theta=0}. \tag{17}$$

In other words, G'_∞ is completely determined by the behavior of the tangential component of the dipolar force, because the radial component is balanced by the repulsive force, irrespective to the detailed form of this repulsive force. Note that G'_∞ still depends on d, where d is still to be determined from the balance of repulsive and dipolar forces. However, if the repulsive force is short ranged as compared to the size of the particle, G'_∞ can be approximated by setting $d=2R$. By doing so, we can derive expressions for the high frequency limit of the storage modulus, making use of Eqs. (9) and (11):

(i) *Saturated regime:*

$$G'_\infty=\frac{\zeta(4)}{4}\mu_0M_s^2\Phi_v, \tag{18}$$

(ii) *Linear regime:*

$$G'_\infty=\frac{3}{4}\mu_0\mu_r\beta^2\zeta(4)\Phi_vH_0^2\left[2\left(1+\frac{\beta\zeta(3)}{2}\right)^{-2}+\left(1-\frac{\beta\zeta(3)}{4}\right)^{-2}\right]. \tag{19}$$

Here Φ_v denotes the volume fraction of particles. The linear dependence on Φ_v is due to the presumed absence of interchain forces.

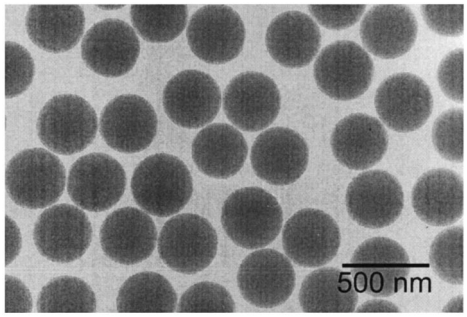

FIG. 2. Electronmicrograph of stearyl silica spheres. The particles shown here have an average radius of 177 nm.

III. EXPERIMENT

A. Model system

1. Silica particles

Silica spheres were synthesized by condensation polymerization of tetra ethoxysilane in an alkaline ethanol/water mixture, following Stöber [16]. The particle radius was determined using static (SLS) as well as dynamic light scattering (DLS). The particle surface was then grafted with octadecylalcohol according to Van Helden, Jansen, and Vrij [6]. Using transmission electron microscopy (TEM), both the particle radius and the polydispersity were determined. The radius of 100 particles was measured. An electronmicrograph of the particles SJL29St (silica Jacob Lopulissa, batch 29, stearylalcohol coated) is shown in Fig. 2. From the density of the suspension (KEM DA200 densitometer) and the mass fraction stearyl silica of the suspension, the density of the particles was calculated. The mass fraction was determined by measuring the dry weight of stearyl silica remaining after drying a known weight of suspension. The density of the particles was used to calculate the volume fraction silica in the samples.

2. Ferrofluid

The stock ferrofluid [coded ffII (ferrofluid, batch II), prepared as described elsewhere [17]] consisted of magnetite particles stabilized by oleic acid, dispersed in cyclohexane. The radius of the magnetite cores was measured using TEM. A Princeton Measurements Corporation Micromag 2900 alternating gradient magnetometer [18] was used to determine the relative magnetization of liquid samples, that is, the magnetization scaled by its saturation value. To determine the saturation magnetization of the ferrofluid the saturation magnetization of a known weight of dried ferrofluid was measured. From this value, the mass fraction ferrofluid particles, and the density of the ferrofluid we could calculate the saturation magnetization of the ferrofluid. Figure 3 shows the full magnetization curve of a liquid ferrofluid sample. This sample consisted of stock ferrofluid diluted with cyclohexane in the same proportion as in the inverse ferrofluid samples (see below), as the magnetization curve of a ferrofluid is concentration dependent [19].

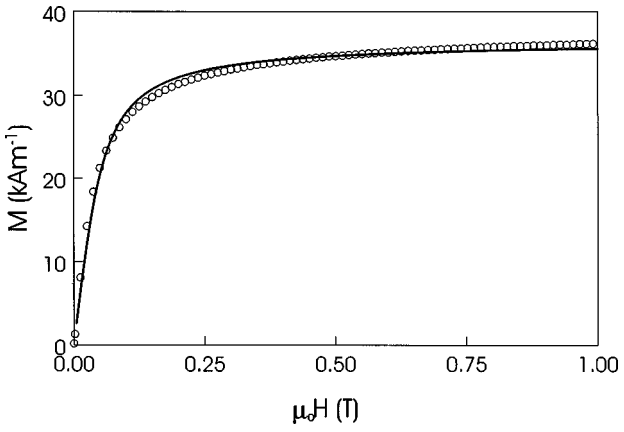

FIG. 3. Magnetization curve of ferrofluid. The drawn line corresponds to the Langevin function fitted to the data.

TABLE I. Characterization of model fluid.

Constituent	Property	Technique	Result
Silica	radius	SLS	190 ± 15 nm
	radius	DLS	205 ± 5 nm
	radius	TEM	177 nm
	polydispersity	TEM	4%
	density		1.804 gr ml^{-1}
Ferrofluid	radius	TEM	5 nm
	saturation magnetization		56.4 kA m^{-1}
	volume fraction		0.34

The values for the mass fraction ferrofluid particles and the density of the ferrofluid were also used to calculate the mass density of the ferrofluid particles, from which the volume fraction could be calculated. The characterization results of the silica and the stock ferrofluid are summarized in Table I.

The rheological properties of a ferrofluid without silica particles may also be affected by a magnetic field, either because it impedes the Brownian rotation of the ferrofluid particles [20] or because it promotes the formation of particle clusters [21]. Therefore, the viscoelastic properties of the stock ferrofluid were measured with the magnetorheometer, as described in the next section. The sample did behave completely viscous in absence and in presence of a magnetic field; no measurable elasticity could be detected. The loss modulus showed a 20% increase in magnetic fields of 245 kA m^{-1}.

3. Sample preparation

Stearyl silica was dried at 70°C in air, in an oven. A concentrated suspension was obtained by dispersing a known weight of dry silica in cyclohexane, using ultrasonication. Inverse ferrofluid samples were then prepared by mixing a concentrated suspension of stearyl silica with the stock ferrofluid. The volume ferrofluid was always chosen such that the ratio of the volume cyclohexane, used to disperse the stearyl silica and the volume ferrofluid, was 1:2. In other words, the magnetization of the ferrofluid surrounding the silica spheres was (approximately) the same for all inverse ferrofluid samples, that is, 37.5 kA m^{-1}. Six samples with different volume fractions silica were prepared, namely 0.031, 0.057, 0.081, 0.126, 0.193, and 0.261.

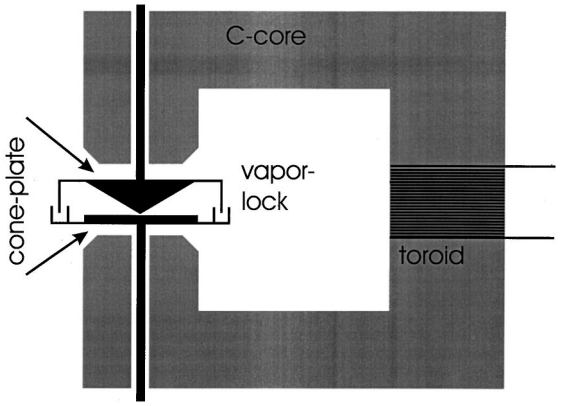

FIG. 4. Schematic drawing of experimental setup.

B. Magnetorheometer

1. Construction of the apparatus

To carry out viscoelasticity measurements on inverse ferrofluids, we had to modify a rheometer, allowing application of a magnetic field. A number of rotational devices has been described in the literature [22–26]. A cone plate geometry has the advantage of constant shear (rate) throughout the gap. On the other hand, Flores *et al.* [27] have found that the structure of a magnetorheological substance may depend on the gap size and rate at which the magnetic field is applied. The gap size depends on the radius in the case of a cone-plate geometry, but is constant for a plate-plate geometry.

A Bohlin VOR rheometer in combination with a laboratory made cone-plate, as well as a plate-plate geometry was used. The cone has a top angle of 1°. Both geometries have a diameter of 6 cm. They are made of nonmagnetic and nonconducting aluminum oxide, to avoid disturbances of the magnetic field and Eddy currents. To prevent evaporation of the volatile cyclohexane, both geometries were provided with an aluminum vapor lock that was filled with ethylene glycol. The contribution of the vapor lock to the measured viscosity was 3 mPa s.

With respect to the magnetic field, Fig. 3 shows that a field strength of 250–300 kA m^{-1} suffices to saturate the ferrofluid. In addition, the field should be homogeneous, not only because we want our magnetic field to be well defined but also to prevent magnetophoresis of nonmagnetic particles. These will move to the regions with the lowest field strength due to the oppositely directed flow of the ferrofluid. These requirements can be met by a toroid in combination with a weak iron *C* core. The power supply of the toroid was controlled by a computer, enabling us to accurately adjust the strength and application rate of the magnetic field. The *C* core was made from Permenorm 5000H3. The air gap was 6 mm. The diameter of the off-rounded cylindrical pole pieces was 5.8 cm, i.e., slightly smaller than the diameter of the cone-plate geometry. This construction is not optimal, because it introduces field inhomogeneities inside the gap. However, without these off-rounded edges the (inverse) ferrofluid tends to leak away from the cone-plate geometry. In the present situation the sample is trapped in a ''magnetic energy sink,'' thereby eliminating the problem. A schematic drawing of the apparatus is shown in Fig. 4. The used power supply limits us to 250 kA m^{-1} at maximum, corresponding to a current of 1.65 A through the toroid, without cooling being necessary. The maximum field inhomogeneity is 4% of its mean value.

2. Magnetic field strength

The magnetic field strength depends on the presence of of a magnetizable sample in the gap between the pole shoes. Modeling the sample as a thin layer of inverse ferrofluid, characterized by a relative permeability $\mu_{r,ffinv}$ and using Ampère's law, the following approximate expression for the magnetic induction B can be derived:

$$B=\frac{\mu_0 Ni}{l_{air}+\dfrac{l_{ffinv}}{\mu_{r,ffinv}}+\dfrac{l_{iron}}{\mu_{r,iron}}}. \tag{20}$$

Here N is the number of windings, i is the current through the toroid, l_{air}, l_{ffinv}, and l_{iron} the path length in air, inverse ferrofluid, and weak iron, respectively, and $\mu_{r,ffinv}$ and $\mu_{r,iron}$ are the relative permeabilities.

The maximum path length through the inverse ferrofluid layer equals the maximum sample thickness, which is 0.53 mm. It can be shown that the error made by omitting the term $l_{ffinv}/\mu_{r,ffinv}$ will never exceed 5%. The following formula for the magnetic field H_{ffinv} inside the inverse ferrofluid sample is obtained:

$$H_{ffinv}\approx\frac{Ni}{\mu_{r,ffinv}\left(l_{air}+\dfrac{l_{iron}}{\mu_{r,iron}}\right)}=\frac{B_{air}}{\mu_0\mu_{r,ffinv}}. \tag{21}$$

In practice, B_{air} was measured in the absence of a sample. H_{ffinv} was calculated by division with $\mu_0\mu_{r,ffinv}$. In a previous paper it was shown that the magnetization (and, consequently, relative permeability) is a linear function of the volume fraction silica particles [28]. So $\mu_{r,ffinv}$ was calculated from the magnetization curve from Fig. 3 and the volume fraction of silica particles, and varied between 2.07 and 1.10.

IV. RESULTS AND DISCUSSION

A. Colloidal stability

The hard-sphere character of the interaction potential between octadecylalcohol coated silica particles in cyclohexane is well established [29]. However, the question seems justified whether the presence of small magnetic particles has any influence on the interaction potential and, consequently, the colloidal stability of the sample. To this end the samples were inspected visually, and their viscosity in the absence of a magnetic field was measured.

The inverse ferrofluid samples did not show any visual sign of colloidal instability. Their appearance was identical to that of ferrofluid without silica particles. Viscosity measurements were performed in the range 10–50 s^{-1} at 25.0 °C, using a Contraves LS40 instrument. The viscosity of a diluted ferrofluid sample having a saturation magnetization identical to that of the ferrofluid medium in the inverse samples was also measured. The samples behaved Newtonian. A relative viscosity was obtained by scaling the viscos-

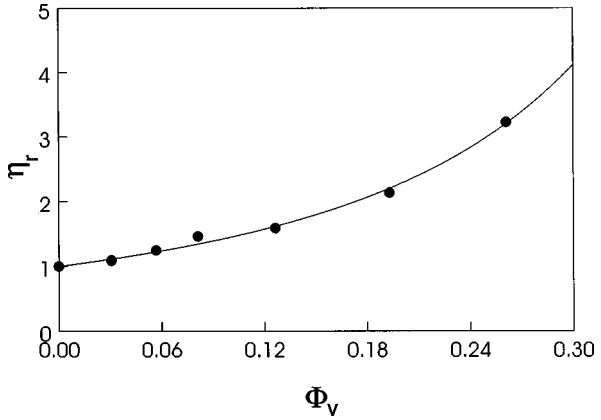

FIG. 5. Viscosity of inverse ferrofluid as a function of the volume fraction silica particles in the absence of a magnetic field. The drawn line corresponds to Quemada's expression for the viscosity of hard spheres, using Φ_{max} as a fitting parameter.

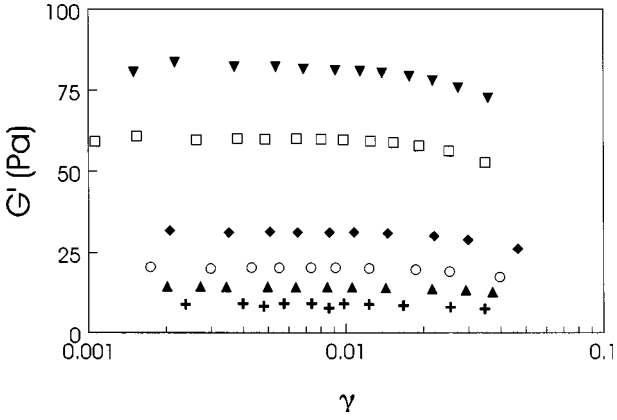

FIG. 7. Storage modulus as a function of the shear deformation amplitude and volume fraction at a field strength of 245 kA m^{-1} and a frequency of 1 Hz. (+ = 0.031, ▲ = 0.057, ○ = 0.081, ◇ = 0.126, □ = 0.193, and ▼ = 0.261).

ity of our inverse ferrofluid samples by the viscosity of the diluted ferrofluid. Data were analyzed using Quemada's expression for the viscosity of hard spheres:

$$\eta_r = \frac{\eta}{\eta_{ff}} = \left(1 - \frac{\Phi_v}{\Phi_{v,max}}\right)^{-2}. \tag{22}$$

Here η_r denotes the relative viscosity, Φ_v denotes the volume fraction of silica particles, and $\Phi_{v,max}$ denotes the maximum volume fraction of silica particles. Equation (22) was fitted to the relative viscosity data, using $\Phi_{v,max}$ as a fitting parameter. The results are shown in Fig. 5. It was found that $\Phi_{v,max} = 0.59 \pm 0.01$, a value close to that of Van der Werff and de Kruif, who found $\Phi_{v,max} = 0.63$ for a system of stearyl silica spheres in cyclohexane. Apparently, the stearyl silica particles still behave as (almost) hard spheres when suspended in ferrofluid.

One would expect depletion attraction between the large silica particles due to the presence of the small (ferrofluid) particles [30]. The hard-sphere behavior of silica particles in ferrofluid can be understood if one assumes that oleic acid–coated ferrofluid particles adsorb onto the surface of the silica particles, as illustrated in Fig. 6. When two silica particles approach each other, the shaded depletion zones from which the small ferrofluid particles are excluded will eventually overlap, giving rise to an entropic force that pushes the silica particles together. However, at the same time that part of the surface of the silica particles that is available for the ferrofluid particles to adsorb on will decrease, giving rise to a force that keeps the particles, separated. When these two forces, mutually cancel, the behavior of the large silica particles will be close to that of hard spheres. The only effect will be an increase of the hydrodynamic radius and, consequently, the effective volume fraction, due to the adsorption of ferrofluid particles. Then the fitting parameter $\Phi_{v,max}$ should decrease, as we indeed observe. The stabilizing effect of adsorbed small particles was also found in sedimentation experiments using mixtures of large and small silica spheres [31].

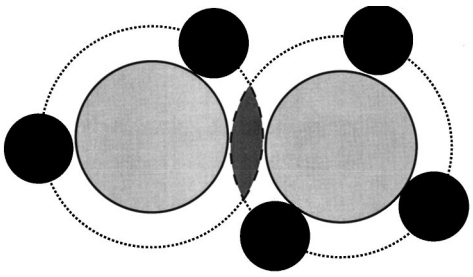

FIG. 6. Small particles are excluded from the gray zone. The surface of this zone is no longer available for particle adsorption.

Since the silica cores cannot penetrate, the thickness of the octadecylalcohol layer, which is approximately 2 nm, can be seen as an upper bound for the difference between $d/2$ and R. The error we make by setting $d = 2R$ is at most 1%.

B. Behavior of the storage modulus

1. Linearity

The linearity was checked by measuring the storage modulus G' as a function of the shear deformation amplitude at a field strength of 245 kA m^{-1} at a frequency of 1 Hz. This field strength corresponds to the magnetic field in air. The results are shown in Fig. 7. G' is nearly constant up to $\gamma = 0.01$, then shows a decrease. For $\gamma > 0.04$, no stable response was obtained, but a steady decrease of G' with time was found. The transition at $\gamma > 0.04$ could be due to the rearrangement of the structures present in the ferrofluid because of mechanical instability. In this context, rearrangement implies either the restructuring of the aggregates to a mechanically stable one or the rupture of the aggregates.

Gulley and Tao calculated the stress response of several chainlike structures upon deformation [32]. It is important to note that in their simulations the particle trajectories were prescribed rather than following from the equations of motion. For single and double chains they found the static modulus decreasing very slowly with an amplitude up to $\gamma = 0.08$. For more complicated structures, such as triple chains and the body centered tetragonal structure, they found strong nonlinear behavior for γ as small as 0.01. Neither of these two extremes is found in our experiment, although our findings do resemble the single chain result more closely. The discrepancy can be explained by the fact that Gulley and

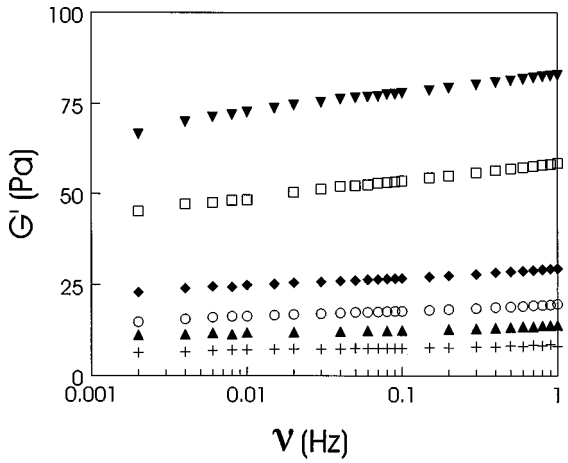

FIG. 8. Storage modulus as a function of frequency and volume fraction at a field strength of 245 kA m^{-1}.

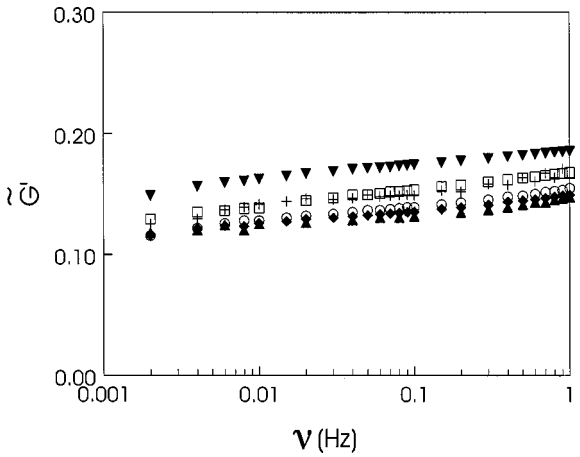

FIG. 9. Storage moduli from Fig. 7 scaled by $\mu_0 \Phi_v M_s^2$.

Tao did not take into account the effect of a finite ranged steric repulsion. The point at which a structure becomes mechanically unstable depends on the range of the sterically repulsive force. Stokesian dynamics simulations of Parthasarathy and Klingenberg [33,34] showed that the point at which mechanical stability occurs strongly decreases with decreasing range of the sterically repulsive part of the potential.

Their simulations also revealed that the observation of a macroscopically linear regime does not imply a linear distortion of the microstructure; slight structural rearrangements occured while the macroscopic response, as averaged over all particles, was still linear. However, incorporating these effects into a simple model, as the one described in Sec. II, is probably not possible.

2. Influence of gap size and application rate

We have compared G' measurements obtained using cone-plate geometry and plate-plate geometry at two different gap sizes, namely 100 and 500 μm. The magnetic field strength was increased at a rate of 250 kA $m^{-1}s^{-1}$, as well as 0.25 kA $m^{-1}s^{-1}$, until the final value of of 245 kA m^{-1} was reached. Within the experimental error no differences were found. Because the cone-plate geometry has the advantage of constant shear throughout the sample, it was used in all other experiments.

3. G' as a function of frequency

G' was measured as a function of frequency in the range 0.002–1 Hz for the six different volume fractions of silica particles at a field strength of 245 kA m^{-1} at which the magnetization is already 90% of the saturation value. The results are shown in Fig. 8. The theory we have developed for the saturated regime suggests a scaling of G' by $\mu_0 \Phi_v M_s^2$, thereby making G' dimensionless. The result is shown in Fig. 9. Considering the reproducibility error in G', which is about 15%, the collapse of the data is consistent with the existence of a single master curve. In other words, up to volume fractions of more than 0.25, G' scales linearly with the volume fraction; at the level of the largest structures, present interaction is negligible. Assuming that these structures are indeed single chains implies that assumption (5) is justified. A linear scaling of magnetorheological properties with Φ_v was also found in other experiments [35].

As can be seen, the G' data show a weak frequency dependence, which is not predicted by our theory. This can be due to different types of deformation of the chains. At high frequency, affine deformation prevails. However, at lower frequencies nonaffine deformation may occur.

4. G' as a function of field strength

G' was measured as a function of field strength for the same six samples as described previously. The measurements were performed at 1 Hz frequency. The choice of frequency was based on the ease with which measurements at higher frequencies can be performed, as compared to lower frequencies. The following measuring procedure was adopted: After insertion of the sample the field was increased stepwise. G' was measured after the signal had become constant. The results are shown in Fig. 10. The magnetic field on the x axis corresponds to that in air. The measured data can now be compared to theoretical predictions. Figure 11 shows the data made dimensionless as follows:

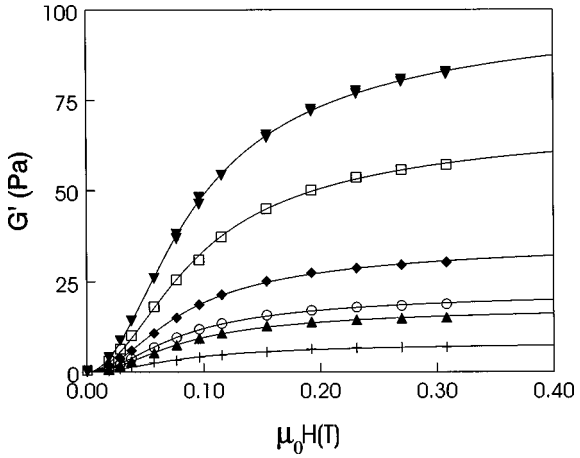

FIG. 10. Storage modulus as a function of field strength and volume fraction at a frequency of 1 Hz. The drawn lines represent squared Langevin functions fitted to the data.

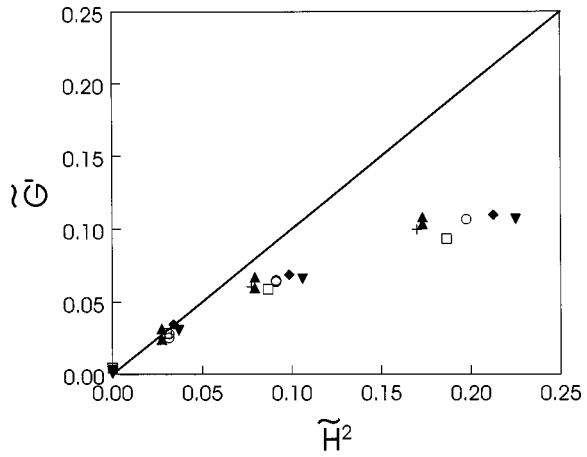

FIG. 11. Storage moduli from Fig. 10 scaled according to Eq. (23). The drawn line represents the linear regime.

$$\tilde{G}' = G'/\frac{3}{4}\mu_0\mu_r\beta^2\Phi_v M_s^2\left[2\zeta(4)\left(1+\frac{\beta\zeta(3)}{2}\right)^{-2} + \zeta(4)\left(1-\frac{\beta\zeta(3)}{4}\right)^{-2}\right]. \quad (23)$$

Similarly, the magnetic field H was scaled by M_s.

Theory overestimates the experimental value for G'. A possible explanation is the discrete nature of the ferrofluid. If the silica particles are at closest contact, the ferrofluid particles are excluded from the gap in between, which leads to a decrease of the induced dipole moment.

As for the saturated regime, the data scaled by $M_o\Phi_v M_s^2$ are shown in Fig. 12. Again the theory overestimates the experimental value for G'. It should be emphasized that at low frequencies the discrepancy between theory and experiment is much larger, as can be seen immediately from Figs. 8 and 9.

Another effect that has not been taken into account is the fact that the chains will seldomly be completely straight. At rest there will be a distribution of chain angles around $\gamma = 0$. The presence of tilted chains will certainly affect G'. This could be checked through simulation studies.

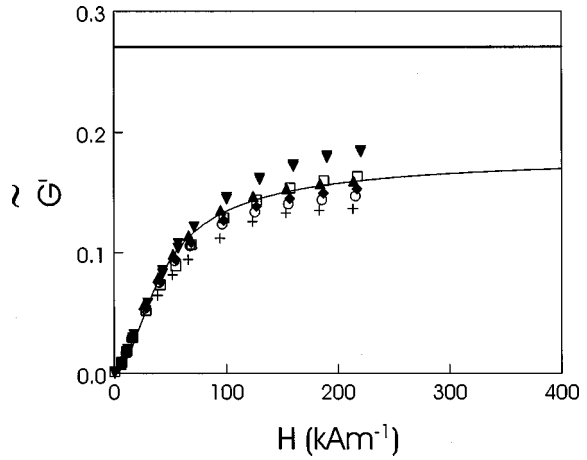

FIG. 12. Storage moduli from Fig. 10 scaled by $\mu_0\Phi_v M_s^2$. The line drawn horizontally represents the saturated regime.

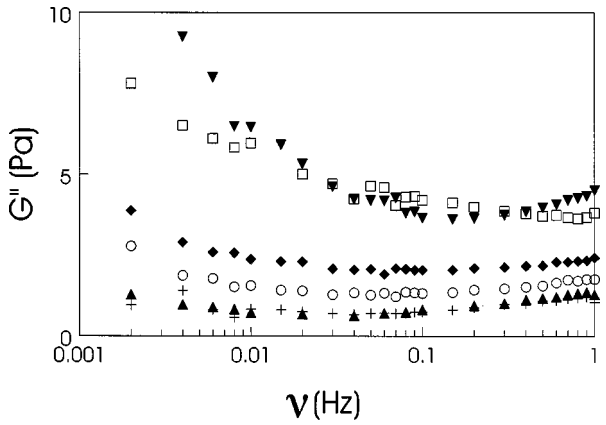

FIG. 13. Loss modulus as a function of frequency and volume fraction at a field strength of 245 kA m^{-1}.

C. Behavior of loss modulus

Up to now no attention has been paid to the behavior of the loss modulus G''. The reason for this neglect is the fact that the ratio G'/G'' is about 10:1 at all field strengths, so that the experimental error in the measured G'' data is of the same order of magnitude as G'' itself. The G'' data equivalent to the G' data discussed in Sec. IV B 3, are shown in Fig. 13. A nonzero G'' could be due to the presence of loose chains, that is, chains of which one or two ends are not connected to the surface of the geometry [36].

V. CONCLUSIONS

We have developed a model magnetorheological fluid consisting of monodisperse silica spheres suspended in an organic ferrofluid. The viscosity of the system in the absence of a magnetic field is very close to that of hard spheres suspended in an effective medium of ferrofluid. The stability of the silica particles against depletion attraction could be due to adsorption of ferrofluid particles at the silica surface. Second, we have developed a magnetorheometer consisting of a commercial instrument equipped with an electromagnet, able to create homogeneous magnetic fields up to 250 kA m^{-1}.

The linear viscoelastic behavior of this ''inverse ferrofluid'' was investigated in the range $10^{-3}-1$ Hz as a function of field strength and volume fraction silica particles. At all field strengths and frequencies the storage modulus G' is an order of magnitude larger than the loss modulus G'': the fluid nearly behaves as an elastic solid. G' shows a weak frequency dependence. G' is linear with volume fraction up to volume fractions of 26% silica particles. A model has been developed to describe the behavior of the high frequency limit of the storage modulus G'_∞. It assumes noninteracting single chains of particles that are deformed affinely. A general formula for the static modulus of such a structure has been derived, taking into account nonmagnetic, repulsive interactions. The magnetic interaction is treated at the dipolar level, incorporating non-nearest neighbor interactions and the effect of finiteness of the chains. At 1 Hz frequency the agreement between theory and experiment is reasonably good.

ACKNOWLEDGMENTS

The stock ferrofluid coded ffII was kindly supplied by Dr. L. Vékás and Dr. D. Bica of the Politehnica University of

Timişoara, Romania. J. Lopulissa is thanked for his help synthesizing the particles SJL29St. E. Altena, G. Beukema, and Dr. V. Shevchenko are thanked for their help constructing the magnetorheometer. The work described in this paper was supported financially by the Stichting voor Fundamenteel Onderzoek der Materie (Foundation for Fundamental Research on Matter), which is part of the Nederlandse Organisatie voor Wetenschappelijk Onderzoek (Dutch Organization for Scientific Research).

APPENDIX: MAGNETIC CONTINUITY OF FERROFLUID

Because the radius of the silica spheres R is only a factor of twenty larger than the magnetite particles, one may question the magnetic continuity of the fluid on the length scale R. In this appendix a measure for magnetic fluctuations is developed.

As the magnetic moment of a nonmagnetic particle is equal, or approximately equal to the total magnetic moment of all ferrofluid particles contained in a spherical volume equal to the size of the nonmagnetic particle, it seems natural to treat the question of magnetic continuity in terms of fluctuations of this total magnetic moment. Chosing the magnetic field along the z axis, the total magnetic moment M can be written as

$$M=\sum_{i=1}^{N} m_z^i. \tag{A1}$$

Here N denotes the number of particles that is present inside the spherical volume and m_z^i denotes the z component of the magnetic moment of a particle. M fluctuates because of the varying number of particles or because of the fluctuating z component of the individual magnetic moments. Assuming negligible magnetic interactions between the ferrofluid particles, so that N and m_z^i are uncorrelated, the mean magnetic moment $\langle M\rangle$ and the variance $\langle \Delta^2 M\rangle = \langle (M-\langle M\rangle)^2\rangle$ can be written as [37]

$$\langle M\rangle = \langle N\rangle \langle m_z^i\rangle, \tag{A2}$$

$$\langle \Delta^2 M\rangle = \langle N\rangle \langle \Delta^2 m_z^i\rangle + \langle m_z^i\rangle^2 \langle \Delta^2 N\rangle. \tag{A3}$$

$\langle\ \rangle$ denotes an ensemble average. As $m_z^i = m\cos\theta$, where θ denotes the angle between the magnetic moment and the z axis, the relative variance can be written as

$$\frac{\langle \Delta^2 M\rangle}{\langle M\rangle^2} = \frac{\langle \Delta^2 \cos\theta\rangle}{\langle N\rangle \langle \cos\theta\rangle^2} + \frac{\langle \Delta^2 N\rangle}{\langle N\rangle^2}. \tag{A4}$$

The importance of fluctuations of $\cos\theta$ decreases with increasing $\langle N\rangle$. From the canonical ensemble it follows that

$$\langle \cos\theta\rangle = \mathcal{L}(\beta\mu_0 mH), \tag{A5}$$

$$\langle \cos^2\theta\rangle = 1 - \frac{2}{\beta\mu_0 mH}\mathcal{L}(\beta\mu_0 mH), \tag{A6}$$

$$\mathcal{L}(x) = \coth(x) - \frac{1}{x}. \tag{A7}$$

Here β denotes $1/k_bT$. Using the grand canonical ensemble, a relation between the isothermal compressibility and the relative fluctuations in the number of particles can be derived:

$$\frac{\langle \Delta^2 N\rangle}{\langle N\rangle^2} = \frac{k_bT}{\langle N\rangle}\left(\frac{\partial\rho}{\partial\Pi}\right)_{T,V}. \tag{A8}$$

Here ρ denotes the number density, Π denotes the osmotic pressure, and V denotes the spherical volume under consideration. For an ideal gas we have

$$\frac{1}{k_bT}\left(\frac{\partial\Pi}{\partial\rho}\right)_{T,V} = 1. \tag{A9}$$

Furthermore, $\langle N\rangle = \Phi_v (R/r)^3$, where r denotes the radius of a ferrofluid particle and R denotes the radius of the spherical volume, which is equal to the radius of a silica particle. Φ_v denotes the volume fraction of ferrofluid particles. The following formula for the fluctuations of the magnetic moment can now be found:

$$\frac{\langle \Delta^2 M\rangle}{\langle M\rangle^2} = \frac{1}{\Phi_v}\left(\frac{r}{R}\right)^3\left[\frac{1}{\mathcal{L}^2(\beta\mu_0 mH)} - \frac{2}{\beta mH\mathcal{L}(\beta\mu_0 mH)}\right]. \tag{A10}$$

It is questionable whether the isothermal compressibility of the ferrofluid is that of an ideal gas. If hard sphere behavior is assumed, the left hand side of Eq. (A9) will be even larger for all concentrations. In that case, Eq. (A10) gives an upper boundary for fluctuations. On the other hand it has been shown that, even in the absence of a magnetic field, the ferrofluid particles tend to form aggregates [38]. This may be due to Van der Waals attraction between the ferrofluid particles. A more careful calculation of the isothermal compressibility of the ferrofluid should take these interactions into account.

It can be seen that Eq. (A10) is a strictly monotonously decreasing function of $\beta\mu_0 mH$. To estimate the magnitude of the fluctuations, we calculate $\sqrt{\langle \Delta^2 M\rangle/\langle M\rangle^2}$ for the lowest and the highest field strength used in the experiments, that is, 8.34 kA m^{-1} and 212 kA m^{-1}. These values correspond to the magnetic field inside the ferrofluid. Data from Table I and the magnetization curve from Fig. 3 were used. The oleic acid layer surrounding the magnetite cores was assumed to have a thickness of 2 nm, that is, r was taken to be 7 nm. For R the SLS radius was used. It was found that at 8.34 kA m^{-1} $\sqrt{\langle \Delta^2 M\rangle/\langle M\rangle^2} = 0.048$, and that at 212 kA m^{-1} $\sqrt{\langle \Delta^2 M\rangle/\langle M\rangle^2} = 0.012$. This implies that at high field strength the fluctuation of the magnetic moment of a nonmagnetic particle can probably be ignored, but that at low field strengths it can be of influence.

A second point of interest related to the continuity is the frequency response of the magnetization of the ferrofluid. When deriving expressions for the self consistent magnetic moment it was assumed that the magnetization reacts instantaneously on a change of the magnetic surroundings. However, the ferrofluid particles have a nonzero magnetic relaxation time, so the question seems justified whether magnetic relaxation plays a role on the time scale at which we per-

formed our viscoelasticity measurements. An indication of the frequency at which magnetic relaxation should be taken into account is given by the Brownian relaxation time τ_b:

$$\tau_b = \frac{3\eta_s V}{k_b T}. \tag{A11}$$

Here η_s denotes the solvent viscosity and V denotes the particle volume. Taking for the solvent viscosity 1 mPa s and a hydrodynamic radius of 10 nm, it follows that $\tau_b = 10^{-6}$ s. This means that, at the frequencies we have studied, magnetic relaxation does not play a role.

[1] W.I. Kordonsky, S.A. Demchuk, and V.A. Kuzmin (unpublished).
[2] A.T. Skjeltorp, Phys. Rev. Lett. **51**, 2306 (1983).
[3] B.E. Kashevsky, W.I. Kordonsky, and I.W. Prokhorov, Magnetohydrodynamics **3**, 368 (1988).
[4] J. Popplewell, R.E. Rosensweig, and J.K. Siller, J. Magn. Magn. Mater. **149**, 53 (1995).
[5] J. Popplewell and R.E. Rosensweig, J. Phys. D **29**, 2297 (1996).
[6] A.K. van Helden, J.W. Jansen, and A. Vrij, J. Colloid Interface Sci. **81**, 354 (1981).
[7] A.P. Philipse and A. Vrij, J. Colloid Interface Sci. **128**, 128 (1989).
[8] R.E. Rosensweig, J. Rheol. **39**, 179 (1995).
[9] G. Bossis, J. Rheol. **41**, 687 (1997).
[10] J.E. Martin and R.E. Anderson, J. Chem. Phys. **104**, 4814 (1996).
[11] J.M. Ginder, L.C. Davis, and L.D. Elie, Int. J. Mod. Phys. B **10**, 3293 (1996).
[12] F. Fujita and T. Mamiya, J. Magn. Magn. Mater. **65**, 469 (1986).
[13] R.P. Sear, Phys. Rev. Lett. **76**, 2310 (1996).
[14] R.E. Rosensweig, *Ferrohydrodynamics* (Dover Press, Mineola, 1997), p. 80.
[15] M. Doi and S.F. Edwards, *The Theory of Polymer Dynamics* (Clarendon Press, Oxford, 1986), p. 72.
[16] W. Stöber, J. Colloid Interface Sci. **26**, 62 (1968)
[17] D. Bica, Rom. Rep. Phys. **47**, 265 (1995).
[18] P.J. Flanders, J. Appl. Phys. **63**, 3940 (1988).
[19] M.I. Shliomis, A.F. Pshenichnikov, K.I. Morozov, and I.Y. Shurubor, J. Magn. Magn. Mater. **85**, 40 (1990).
[20] J.P. McTague, J. Chem. Phys. **51**, 133 (1969).
[21] S. Odenbach and H. Störk, J. Magn. Magn. Mater. **183**, 188 (1998).
[22] Y. Grasselli, G. Bossis, and E. Lemaire, Prog. Colloid Polym. Sci. **93**, 175 (1993).
[23] M. Schott, L. Vékás, and D. Bica, Rom. Rep. Phys. **47**, 411 (1995).
[24] H.M. Laun, C. Kormann, and N. Willenbacher, Rheol. Acta **35**, 417 (1996).
[25] Z.P. Shulman, V.I. Kordonsky, E.A. Zaltsgendler, I.V. Prokhorov, B.M. Khusid, and S.A. Demchuk, Int. J. Multiphase Flow **12**, 935 (1986).
[26] H. Janocha and B. Rech, Rheology **4**, 198 (1994).
[27] G.A. Flores, M.L. Ivey, J. Liu, M. Mohebi, and N. Jamasbi, in *Proceedings of the 5th International Conference on Electrorheological Fluids, Magnetorheological Suspensions and Associated Technology, Sheffield, 1995*, edited by W.A. Bullough (World Scientific, Singapore, 1996), p. 494.
[28] B.J. de Gans, C. Blom, J. Mellema, and A.P. Philipse, J. Magn. Magn. Mater. **201**, 13 (1999).
[29] A. Vrij, J.W. Jansen, J.K.G. Dhont, C. Pathmamanoharan, M.M. Kops-Werkhoven, and H.M. Fijnaut, Faraday Discuss. Chem. Soc. **76**, 19 (1983).
[30] J.S. van Duijneveldt, A.W. Heinen, and H.N.W. Lekkerkerker, Europhys. Lett. **21**, 369 (1993).
[31] D.M.E. Thies-Weesie, A.P. Philipse, and H.N.W. Lekkerkerker, J. Colloid Interface Sci. **177**, 427 (1996).
[32] G.L. Gulley and R. Tao, Phys. Rev. E **48**, 2744 (1993).
[33] M. Parthasarathy and D.J. Klingenberg, Rheol. Acta **34**, 417 (1995).
[34] M. Parthasarathy and D.J. Klingenberg, Rheol. Acta **34**, 430 (1995)
[35] X. Tang and H. Conrad, J. Rheol. **40**, 1167 (1996).
[36] T.C.B. McLeish, T. Jordan, and M.T. Shaw, J. Rheol. **35**, 427 (1991).
[37] A.W. Drake, *Fundamentals of Applied Probability Theory* (McGraw-Hill, New York, 1967), p. 109.
[38] L.N. Donselaar, Ph.D. thesis, Utrecht University, 1998.